CPW-fed band-notch ultra-wideband antenna with Cyrillic Ghe-shaped parasitic slit

R. AZIM[1,*], M. S. MIA[1], A. K. M. ARIFUL HAQUE SIDDIQUE[1], M. MOTTAHIR ALAM[2], M. TARIQUL ISLAM[3]
[1]*Department of Physics, University of Chittagong, Chattogram 4331, Bangladesh*
[2]*Department of Electrical and Computer Engineering, Faculty of Engineering, King Abdulaziz, Jeddah 21589, Saudi Arabia*
[3]*Department of Electrical, Electronic and Systems Engineering, Universiti Kebangsaan Malaysia, 43600 Bangi, Malaysia*

A CPW-fed ultra-wideband antenna with a notched band for WLAN is presented in this paper. A hexagonal patch, a feedline, and a pair of coplanar grounds constitute the antenna on the plane of a substrate. A Cyrillic Ghe-shaped parasitic slit is added within the inverted U-shaped ground to filter out the WLAN band. The theoretical and measured results confirm that the patch matched well with grounds that helped the antenna achieve the UWB working band. On the other hand, the filter element helped the design to generate a notched band of 5.05 – 5.86 GHz. The antenna achieved good gain and efficiency and exhibited flat group delay except at the notch band. Moreover, the engineered antenna demonstrates nearly omnidirectional radiation patterns. To exhibit the perspective of the planned antenna, it is compared to the formerly reported UWB antennas with a WLAN notch band.

(Received December 19, 2023; accepted June 3, 2024)

Keywords: UWB antenna, Notch band, WLAN, Filter element, Wireless communication

1. Introduction

After the FCC allocated the 3.1 to 10.6 GHz band to the unlicensed civil ultra-wideband (UWB) technology, UWB has received much user attention. The UWB technology possesses high transmission efficiency, high processing gain, good concealment, high multipath resolution, low cost, and low power consumption. It is widely used in high-precision positioning, high-speed multimedia wireless communication, radar, sensors, control, microwave medical imaging, and other fields. As an essential part of UWB technology, the research on ultra-wideband antennas mainly focuses on the conventional operating band and the antenna size, where microstrip planar antennas possess significant advantages over other antennas. For example, the antenna reported in [1] uses a series of triangular slots in the ground to raise the bandwidth by 43.6 % compared to that without the slots. The UWB antenna reported in [2] achieved an operating band of 2.96 – 19 GHz, and the bandwidth was extended by increasing resonant modes using an asymmetric patch and offset feeding. The achieved working band of this antenna has a bandwidth of 146%, which is 115.5% better than that of the conventional patch antenna.

A vital issue of ultra-wideband technology is the electromagnetic interference with the narrow wireless bands that coexist inside the designated band of 3.1 to 10.6 GHz. For example, the wireless local area network (WLAN) operating over 5.15 – 5.85 GHz may interfere with the UWB band. The band notch function is mandatory to mitigate the interference caused by narrowband signals. The commonly used methods to achieve band-notch function are the use of split-ring resonators (SRRs), etching geometric slots of different shapes, the addition of parasitic slits/cells, and the addition of resonant branches [3-7]. For example, using a pair of split ring resonators, the antenna reported in [3] filtered out the 5.12 – 6.77 GHz WLAN band from the UWB working band of 2.44 – 10.79 GHz. However, the realized notched band of this antenna is wider than the designated WLAN band, and it possesses a bigger dimension of 78 mm × 44.6 mm. For band notch UWB communication, a circular patch antenna with a 30 mm × 40 mm dimension is reported in [4] that employs a quarter wave transfer matching technique to have the 2.4 to 13.8 GHz band. It uses four rectangular SRRs in the radiator to produce a notched band centered at around 5.6 GHz. In [6], Chen et al. proposed a band-notch UWB antenna. It is composed of a ring-shaped patch having triple matching elements, a transition element, and two rectangular ground planes and is etched on an FR4 substrate of 26 mm × 34 mm. Here, a T-shaped construct is embedded within the ring radiator to generate a notched band of 4.8 – 5.8 GHz, wider than the designated band. A circular UWB antenna with a reconfigurable notched band is reported in [7]. In this design, an indefinite L-type slot is cut in the ground to reject a band ranging from 3.89 to 5.93 GHz. But it has a relatively big footprint of 38.87 mm × 24 mm, and the notched band is quite large. Ref. [11] reported a transparent UWB antenna with a single trap band. Using a pair of SRRs beside the circular radiator, this antenna with an area of 30 mm × 30 mm realizes a notched band of 5 – 6 GHz. A CPW-fed UWB antenna with a WLAN notch band is reported in [12]. To generate a controllable notch band, it parallelly added two half-wave stubs near the edge

of the tapered-shaped slot and etched one slit within the patch. A miniature UWB antenna having a WLAN notch band is reported in Ref. [13]. Having an area of 840 mm^2, it uses a half-wavelength thin strip dipole to reject a spectrum of 5 to 6 GHz, which is higher than the allocated WLAN band. A CPW-fed single-layer band notch antenna with a size of 30 mm × 28 mm is reported in [14]. In this design, two open-ended half-wave-length stubs and two slits are placed within the slotted ground and circular patches to reject a band ranging from 5.2 to 6.0 GHz. Ref. [15] presents a balanced circular UWB antenna with filtering capability. The antenna comprises a stub-loaded circular radiating element and uses a pair of spur-lines of quarter wavelength in the differential feedline to achieve band-notch characteristics. Despite the WLAN filtering capability, its notched band (5.01 – 6.19 GHz) is larger than the required band of 5.15 to 5.85 GHz. A 24 mm × 30 mm fan-shaped circular slot ultra-wideband antenna with a WLAN notch band is proposed in [16]. Adding a U-shaped slit on top of the ground, this design filtered out the 5.0 – 5.85 GHz band. A hexagonal antenna with a WLAN notch band is presented in [17]. Here, two C-shaped stubs are placed beside the feedline and filtered out the 4.5 – 5.85 GHz band, which is higher than the required WLAN band. In [18], a band-notch UWB antenna is reported for body-centric communication. This swan-shaped antenna filtered out the 4.5 to 6.1 GHz with the help of a U-shaped narrow slot on the feedline. However, the acquired notched band is quite large compared to the required band of WLAN. A band-notch UWB annular ring antenna with a stop band of 5.1 – 5.95 GHz is presented in [19]. In this design, the notched band was generated by adding a disc-shaped slot on the lower side of the patch. In [20], a UWB antenna with the WLAN notch band is presented. By truncating the lower parts of the radiator, the presented antenna achieved the UWB band. In contrast, the notch band was generated using EBG structures composed of a pair of metallic conductors. However, the span of the acquired stop band is 5 – 6 GHz. The UWB antenna reported in [21] uses an L-type slot in the patch to create a notched band to avoid interference caused by the WLAN band. However, the bandwidth of the rejected band (5.1 to 6.1 GHz) is relatively wider. Though most of the reported antennas filtered out the WLAN to avert the interference between UWB and WLAN, they possess a large size and complex footprint. Moreover, some antennas filtered out the frequency band, which is larger than the required WLAN band (5.15 – 5.85 GHz), resulting in degradation of the signal quality.

For the UWB application with notch characteristics, this article presents a CPW-fed uniplanar antenna. This simple antenna comprises a hexagonal radiator and a pair of modified ground planes and is fabricated on the same side of FR4 material. To have a notched band at around 5.5 GHz, one Cyrillic Ghe-shaped filter element is placed within the ground plane. The combined effect of the patch, ground planes, and filter elements helps the antenna work over the entire UWB spectrum with a stop band of 5.05 to 5.86 GHz. The antenna structure is straightforward, uni-planar, inexpensive, easy to mass-produce, and achieves an ultra-wide working band. Moreover, it has a dimension of 24.5 × 20 mm^2 and is much smaller than many band-notch antennas reported in the open literature.

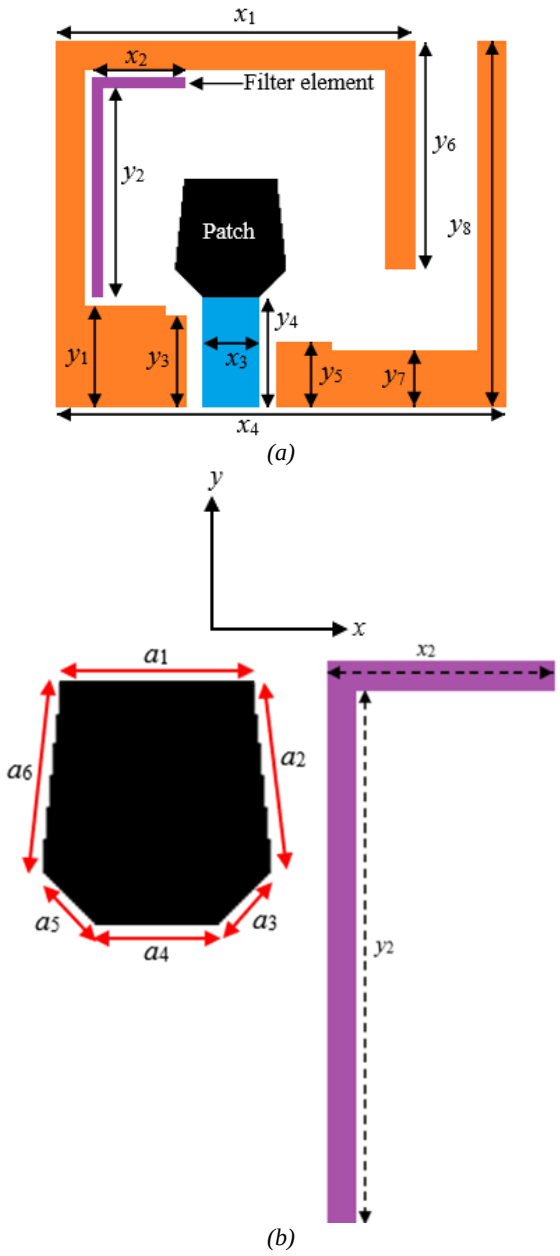

Fig. 1. (a) Antenna footprint, (b) hexagonal-shaped patch, and Cyrillic Ghe-shaped filter element (color online)

2. Antenna design

2.1. Antenna geometry

The footprint of the planned antenna is portrayed in Fig. 1. It consists of a hexagonal-shaped radiator, a microstrip line, and two asymmetric ground planes. The hexagonal-shaped radiating element and the ground planes are engineered on the same side of a single-sided FR4 substrate having a thickness of 1.6 mm, a permittivity of 4.6, and a copper metallization of 35 microammeters. A

50Ω SMA is connected to feed the antenna, which is also considered during the simulation. To have an operating band to cover the entire UWB spectrum, the shape, position, and size of the patch and ground planes are optimized using EM simulator IE3D. From the S-parameter portrayed in Fig. 2, it can be commented that the hexagonal-shaped radiator strongly coupled with the grounds and the antenna without filter element realized an impedance band of 3.08 GHz to 11 GHz.

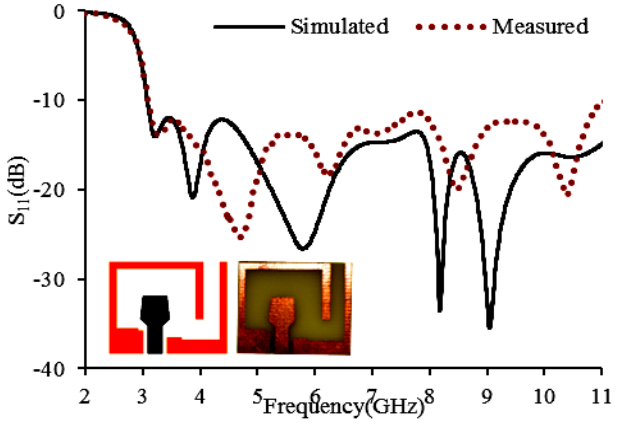

Fig. 2. S_{11} response of the antenna without filter element (color online)

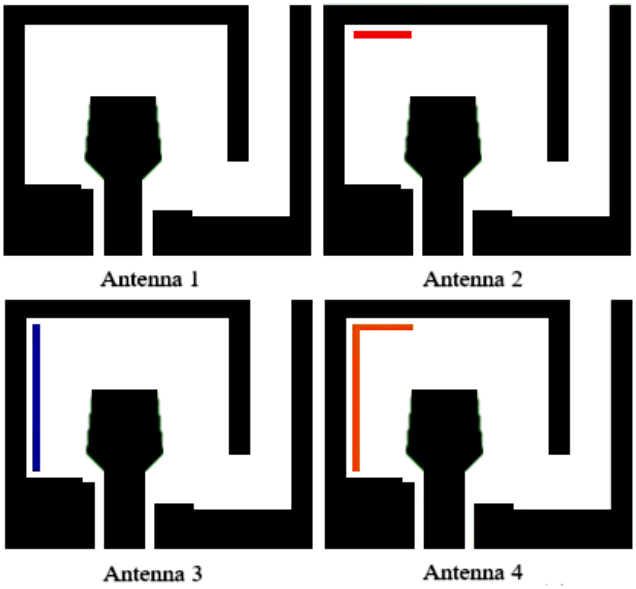

Fig. 3. Different evolution stages (color online)

2.2. Design evolution of band-notch antenna

To comprehend the achieving of the desired band notch characteristics, the evolution stages of the studied antenna are portrayed in Fig. 3 and Fig. 4. As in Fig. 4, the primary antenna (antenna-1) with the hexagonal-shaped patch and two asymmetric grounds achieves an ultra-wide operating band of 3.08 to more than 11 GHz where its impedance very much close to 50 ohms. When a rectangular slit of 4.5mm × 0.5mm is horizontally placed within the ground plane to form antenna-2, it still exhibits the UWB characteristics as in Fig. 4(a). The vertical placement of a rectangular slit of 0.5mm × 12mm forming antenna-3 demonstrates a notched band at around 6.9 GHz, as in Fig. 4(a), and failed to filter the 5.5 GHz band for WLAN. Fig. 4(b) also reveals that, at 6.9 GHz, the characteristic impedance is far from 50 ohms. Finally, when the Cyrillic Ghe-shaped parasitic slit is inserted within the ground planes (antenna-4), a notched band at 5.5 GHz is produced, as observed in Fig. 4(a), and the antenna can minimize the interference caused by WLAN. As seen from Fig. 4(a) that a single trap characteristic of WLAN is achieved by etching a Cyrillic Ghe-shaped parasitic slit within the modified ground plane.

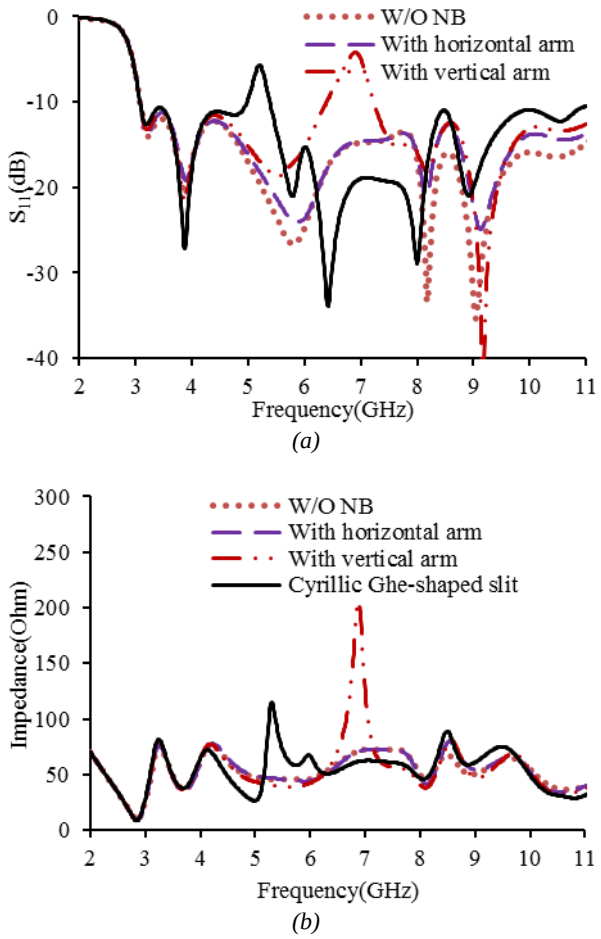

Fig. 4. S_{11} and Z-parameter for different evolution stages (color online)

The mathematical formula estimates the length of the slit is [8]

$$L = \frac{c}{2f_{notch}\sqrt{\varepsilon_e}} \quad (1)$$

where c is the light velocity, ε_e is the effective permittivity, and f_{notch} is the center frequency of the notch band. The effective permittivity ε_e can be calculated using [8]

$$\varepsilon_e = \frac{\varepsilon_r + 1}{2} \quad (2)$$

and therefore, the slit length corresponding to the center frequency of the notch band is [8]

$$L_{notch} = \frac{c}{f_{notch}\sqrt{2(\varepsilon_r + 1)}} \approx x_2 + y_2 \quad (3)$$

where x_2 and y_2 are the parameters of the slit. The calculated length of the slit using (3) is 16.3 mm, whereas the actual length of the slit is 16.5 mm, which is very much close to the calculated length. All the parameters of the designed antenna are listed in Table 1.

Table 1. Parameters of the proposed antenna

Parameter	Value(mm)	Parameter	Value(mm)
x_1	19.5	y_6	12.5
x_2	5.0	y_7	3.0
x_3	3.0	y_8	20
x_4	24.5	a_1	5.0
y_1	5.5	a_2	5.02
y_2	11.5	a_3	2.12
y_3	5.0	a_4	3.0
y_4	6.5	a_5	2.12
y_5	3.5	a_6	5.02

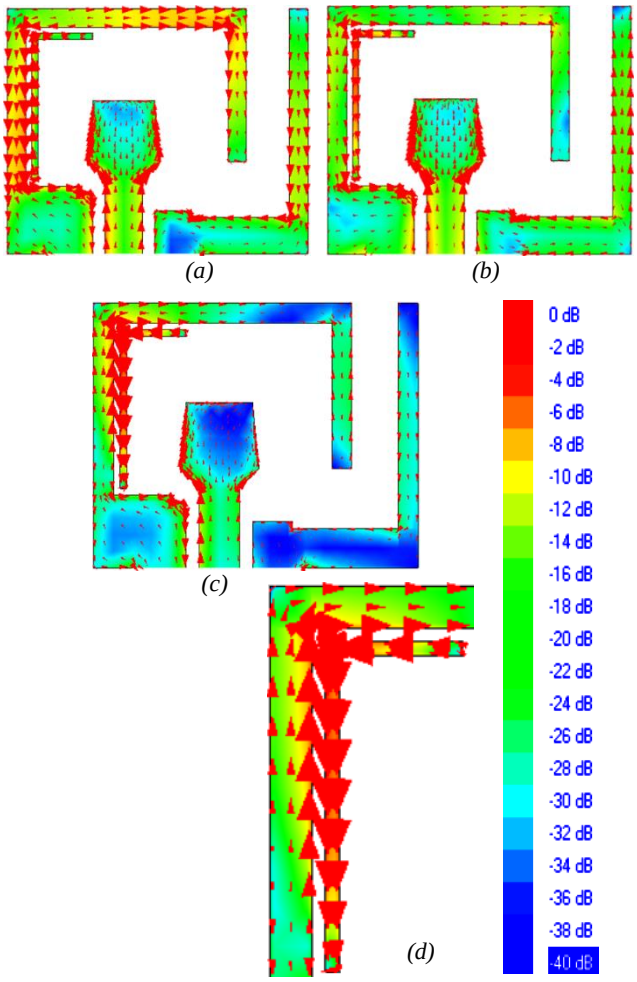

Fig. 5. Current distribution at (a) 3.88 GHz (passband), (b) 6.42 GHz (passband), (c) 5.55 GHz (notch band), and (d) enlarged view of current on the filter element at 5.55 GHz (color online)

To demonstrate the creation of a notched band, the surface current distributions on the antenna at passband frequencies of 3.88 GHz and 6.42 GHz and notch band frequency of 5.55 GHz are portrayed in Fig. 5. It is seen that at passband frequencies, the currents are almost uniformly distributed over all parts of the antenna including Cyrillic Ghe-shaped filter element that is all parts radiate the power almost uniformly. On the other hand, at 5.55 GHz (notch frequency), compared to the different parts of the antenna, the current is primarily distributed around the Cyrillic Ghe-shaped slit, and the intensity is higher on the slit. Moreover, the direction of the current flow in the slit is opposite to that of adjacent ground plane arms, as portrayed in Fig. 5(d). This opposite flow of currents suppressed the radiated power, creating a stop band and a drastic decrement in antenna gain and efficiency at the 5.5 GHz band.

3. Results and discussion

3.1. Frequency-domain characteristics

With the help of perceptive analysis and current distribution, a truthful overview of the planned antenna performance is achieved. The designed antenna is then built to validate computed results. The antenna prototype is portrayed in Fig. 6, and its S_{11} is measured through the 50-ohm port of the network analyzer (Agilent N5227A). Fig. 7 displays the simulated and physical measurement results of the S-parameter. As seen in Fig. 7, for $S_{11} \leq -10$ dB, the antenna realized an impedance band of 3.08 – 10.81 GHz with a stop band ranging from 5.05 to 5.86 GHz. As in Fig. 7, a diffuse difference between the computed and measured results has been observed. These differences are primarily due to soldering inaccuracy and prototype tolerance.

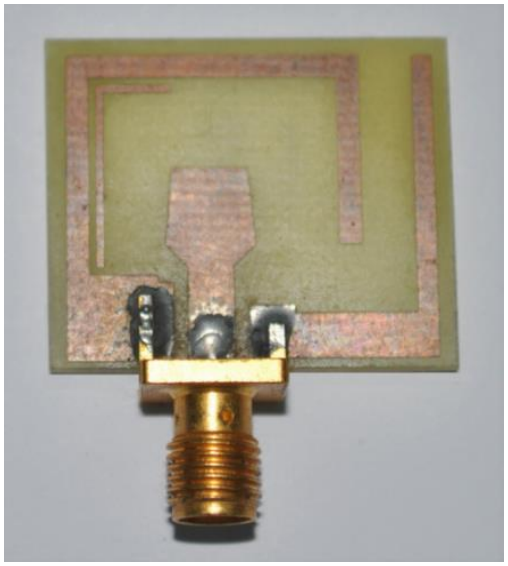

Fig. 6. A photograph of the fabricated antenna (color online)

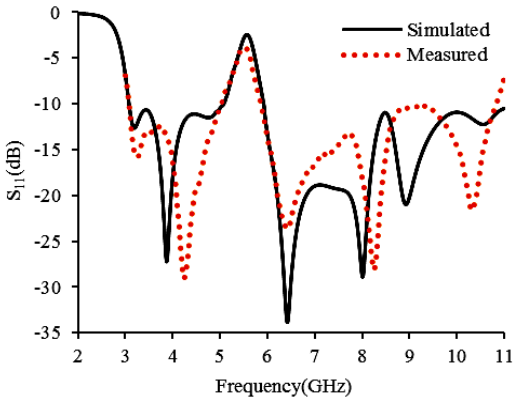

Fig. 7. Simulated and measured S_{11} of the antenna (color online)

The simulated and measured 2D gain is illustrated in Fig. 8, while Fig. 9 portrays the radiation efficiency. The measurement was carried out in MVG's StarLab near-field anechoic chamber, which can measure the spectrum from 650 MHz to 18 GHz. As seen in Fig. 8, the antenna achieved good gain except in the notched band. The designed band notch antenna also achieved good radiation efficiency with a sharp decrement in the WLAN notch band, as shown in Fig. 9. The drastic fall of gain and efficiency in the WLAN spectrum is due to the weak radiation from the antenna at that band.

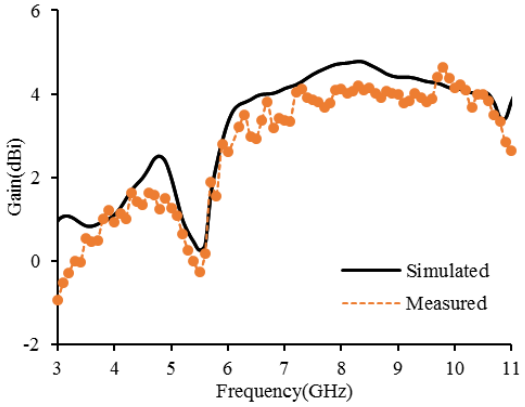

Fig. 8. Peak gain in the operating band (color online)

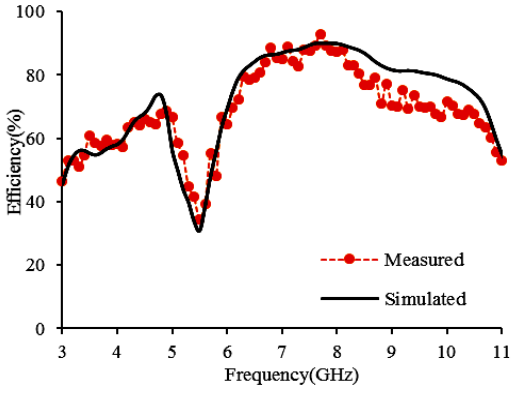

Fig. 9. Radiation efficiency in the operating band (color online)

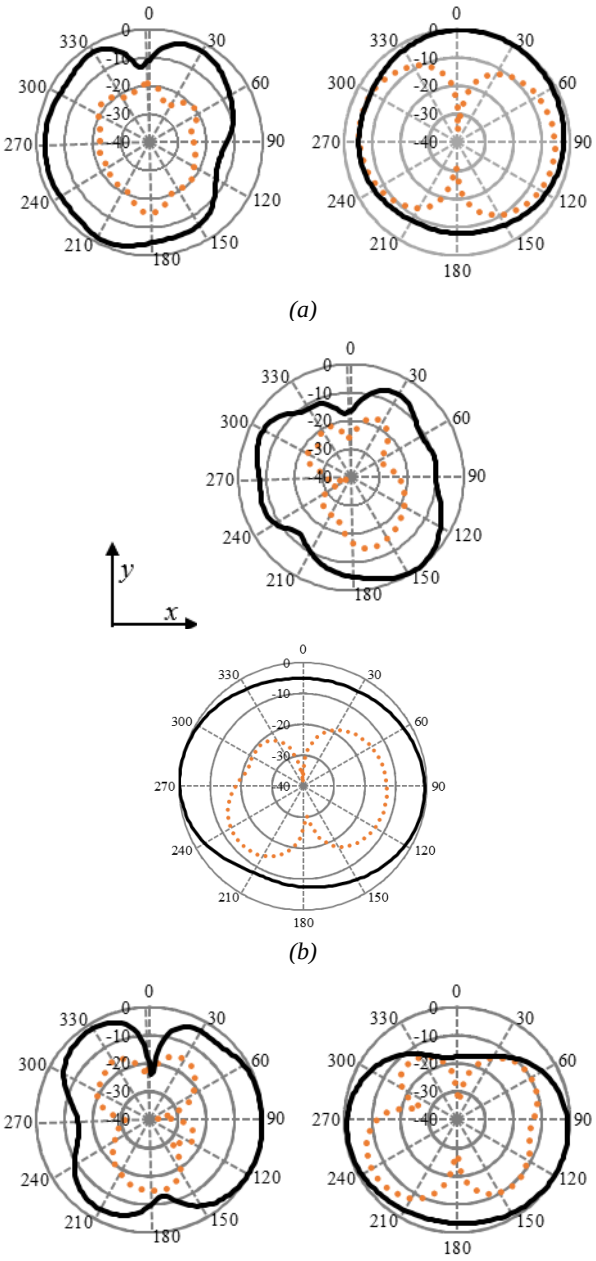

Fig. 10. Measured E-plane (left), and H-plane (right) patterns at (a) 3.8, (b) 6.4, and (c) 8.9 GHz. The solid black lines represent the co-polarized components, and the orange dashed lines represent the cross-polarized components (color online)

The 2D radiation characteristics are simulated and measured at some selected frequencies and are portrayed in Fig. 10. As seen in Fig. 10, the pattern is quite omnidirectional at lower frequencies. At low frequencies, a higher cross-polarization level is observed in the H-plane pattern, which may be due to the excitation of surface waves in the ground planes [22-23]. When the surface propagates and strikes the edges of the ground planes, they are reflected and diffracted. These diffracted waves increase the resultant radiation, produce distortion in the waves, and increase the cross components. At the higher

frequency, the patterns become slightly directional with dips. Although high cross-polarization is observed at a lower frequency, the figure reveals that the radiation behavior of the designed antenna is symmetric and omnidirectional, which is an essential requisite of UWB communication application.

3.2. Time-domain characteristics

As the UWB antenna transmits narrow pulses instead of continuous waves and only frequency domain results cannot ensure the suitability of the anticipated antenna for UWB application, it is necessary for an antenna to possess good time domain behavior. To explore time-domain characteristics, fidelity factor (FF), group delay, transmission coefficient (S_{21}), and phase of S_{21} are analyzed. The simplest method to test the time domain characteristics is the fidelity factor that correlates the transmitting and receiving signals. The FF is determined by placing two identical antennas, transmitter and receiver, and equation (4) is usually used [24]

$$FF = Max\left[\frac{\int T_x(t)R_x(t-\tau)dt}{\sqrt{\int T_x^2(t)dt}\sqrt{\int R_x^2(t)dt}}\right] \quad (4)$$

with input pulse T_x and received pulse R_x. The FF is calculated using an EM simulator where a Gaussian pulse is taken as input, and 10 virtual probes are placed in the far-field region. The angular separation between the two probes is 10º, and the distance between the two antennas is fixed at 240 mm in face to face. The waveform of input and received signals is portrayed in Fig. 11(a). It is revealed that the FF of the studied antenna is 88.5%, which is very close to the minimum acceptable FF of 90% [25].

The group delay of the presented antenna that specifies the distortion of the signal is portrayed in Fig. 11(b). From the plot, it is confirmed that the designed antenna exhibits a flat group delay except at the notched band, proving the planned antenna's suitability in UWB applications. The measured and simulated values of the transfer function, S21, are portrayed in Fig. 11(c). Despite some ripples, the measured value matched well with the theoretical one. The nulls in the S_{21} curves are due to the impedance mismatch at these points. The phase variation of the S_{21}, as in Fig. 11(d), demonstrates that the phase is almost linear throughout the operating band except at the notch band. This flat variation of the phase reveals that the studied antenna does not distort the input and output pulses phase.

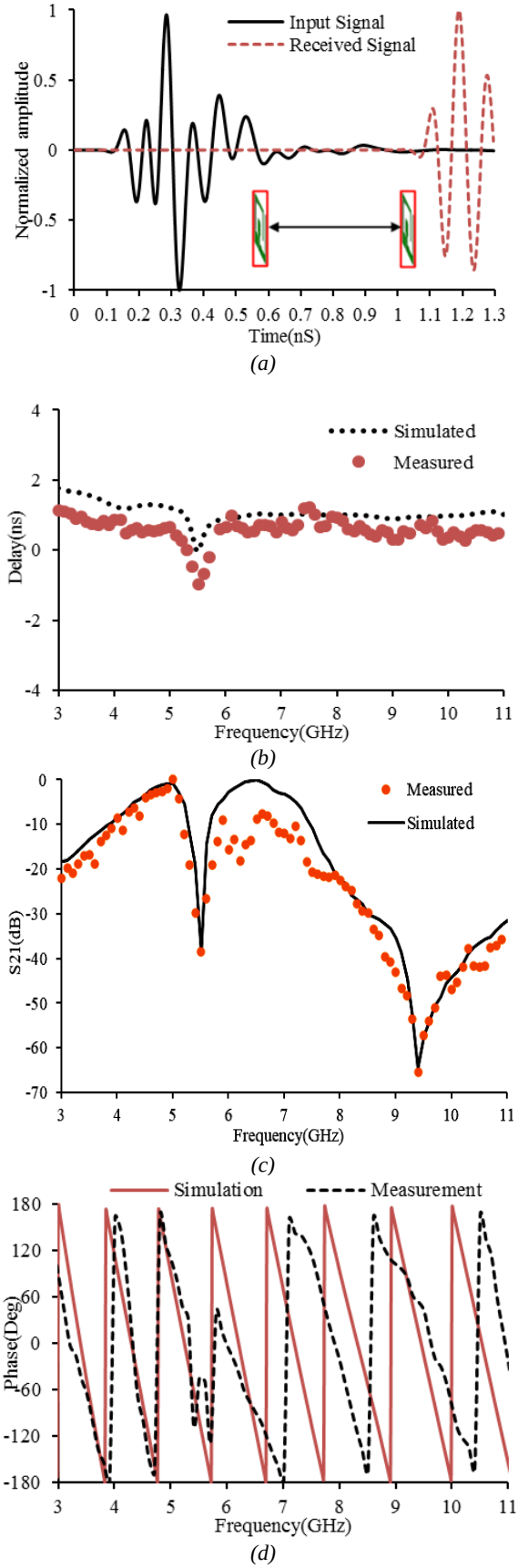

Fig. 11. (a) Normalized input and received signal, (b) group delay, (c) S_{21}, and (d) phase of S_{21} in the UWB band (color online)

In Table 2, the performance of the designed antenna is compared with previous works on band-notch UWB antennas in terms of size, notched band, and filtering techniques. It is revealed that almost all the reported antennas with WLAN notched bands are relatively larger than the proposed one. Moreover, the bandwidth of some of the antenna's notched bands is wider than the designated WLAN band of 5.15 – 5.85 GHz. Table 2 shows that the engineered antenna outperformed the existing WLAN notch UWB antennas in terms of simple footprint, small size, and bandwidth of the notched band.

Table 2. Comparison of the performances of some band-notch UWB antennas

Ref.	Year	Dimension (mm×mm)	Area (mm^2)	Notch band (GHz)	Substrate, ε_r	Filter element
[6]	2014	26×34	1060	4.80–5.80	FR4, 4.4	T-shaped construct
[14]	2014	30×28	840	5.20–6.00	NR, 2.55	Tapered slot and slits
[11]	2015	30×30	900	5.00–6.00	AgHT8, 3.228	Circular SRR
[3]	2016	78×44.6	3479	5.12–6.77	FR4, 4.4	Slot-type SRR
[4]	2016	30×40	1200	5.15–5.85	FR4, 4.4	Rectangular SRR
[13]	2016	28×30	840	5.00–6.00	FR4, 4.4	Thin strip dipole
[15]	2017	29.38×28.25	830	5.01–6.19	RO4003, 3.55	Pair of spur-lines
[12]	2018	30×28	840	5.00–5.80	Taconic, 2.55	Slot and stubs
[16]	2019	24×30	720	5.00–5.85	FR4, 4.3	Inverted U-shaped slit
[17]	2019	21.25×32.75	696	4.5–5.85	Teflon, 2.1	C-shaped stubs
[7]	2020	38.87×24	933	3.89–5.93	FR4, 4.4	L-shaped slot
[26]	2021	25×30	750	5.15–6.00	FR4, 4.4	Vertical stub
[27]	2021	60×58	3480	5.30–6.00	FR4, 4.3	Rectangular slit
[18]	2022	25 ×25	625	4.50–6.10	RO4003C, 3.55	U-shaped slot
[28]	2022	23 ×28	644	5.00–6.30	FR4, 4.4	U-shaped slot
[29]	2022	30×24	720	5.15-5.825	FR4, 4.4	symmetrical meandering strips
[30]	2022	44.1×60	2646	4.32–5.96	F4B, 2.94	Double SRR
[31]	2023	60×62	690	5.15–5.725	Kaptom, 3.5	Triangular-shaped spiral slot
This work	**2023**	**24.5×20**	**490**	**5.05–5.86**	**FR4, 4.6**	**Cyrillic Ghe-shaped slit**

4. Conclusion

This paper proposes a UWB antenna that notches a frequency band used by WLAN. To create the notch band at 5.5 GHz, a Cyrillic Ghe-shaped slit has been added along with the hexagonal patch and two ground planes as a filter element. The current distribution on the slit reveals that at 5.5 GHz, currents dominate at the filter element and oppose the main radiator currents, resulting in a notched band of 5.05 to 5.86 GHz within the UWB spectrum. The planned antenna has good gain and efficiency, exhibits stable radiation characteristics and time domain behaviors, and is very fit for UWB communication systems.

Acknowledgments

Research and Publication Cell of the University of Chittagong, Bangladesh, sponsoring this work under grant number 1108)/2022-23/2nd Call/08/2023.

References

[1] R. Azim, M. T. Islam, N. Misran, Appl. Comput. Electromagn. Soc. J. **26**, 856 (2011).
[2] R. Azim, R. W. Aldhaheri, M. M. Sheikh, M. T. Islam, Microw. Opt. Technol. Lett. **58**, 1221 (2016).
[3] L.-C. Tsai, W-J. Chen, Microw. Opt. Technol. Lett. **58**, 2595 (2016).
[4] G. Mishra, S. Sahu, Microwave and Optical Technology Letters **58**, 1068 (2016).
[5] R. Azim, M. T. Islam, A. T. Mobashsher, IEEE Antennas Wirel. Propag. Lett. **12**, 1412 (2013).
[6] A. Chen, C. Yang, Z. Chen, K. A. N, J. Fang, W. Jiang, Appl. Comput. Electromagn. Soc. J. **29**, 134 (2014).
[7] A. De, B. Roy, A. K. Bhattacharjee, Int. J. Commun. Syst. **33**, e4323 (2020).
[8] A. K. M. A. H. Siddique, R. Azim, M. T. Islam, Int. J. Microw. Wirel. Technol. **11**, 711(2019).
[9] M. A. Dorostkar, R. Azim, M. T. Islam, Proc.

Technol. **11**, 1285(2013).
[10] M. Shuhrawardy, M. H. M. Chowdhury, R. Azim, 2019 International Conference on Electrical, Computer and Communication Engineering, 7 - 9 Feb 2019, Bangladesh.
[11] M. S. A. Rani, S. K. A. Rahim, P. J. Soh, B. M. Saad, M. I. Sabram, M. F. M. Yusoff, Appl. Comput. Electromagn. Soc. J. **30**, 1215 (2015).
[12] M. Shi, L. Cui, H. Liu, et al., Prog. Electromagn. Res. M. **74**, 201 (2018).
[13] W. Ding, G. Wang, Microw. Opt. Technol. Lett. **58**, 2780 2016).
[14] Z.-H. Tu, W.-A. Li, Q.-X. Chu, IEEE Antennas Wirel. Propag. Lett. **13**, 1296 (2014).
[15] C. H. Lee, J. H. Wu, C.I G. Hsu, H. L. Chan, H. H. Chen, IEEE Antennas Wirel. Propag. Lett. **16**, 2812 (2017).
[16] V. N. K. R. Devanaa, A. M. Rao, Int. J. Electron. Lett. **7**, 352 (2019).
[17] A. Bhattacharya, B. Roy, S. K. Chowdhury, A. K. Bhattacharjee, Indian J. Pure Appl. Phys. **57**, 272 (2019).
[18] S. R. Ahasan, K. Islam, M. M. Khan, M. Masud, G. S. Gaba, H. A. Alhumyani, Comput. Syst. Sci. Eng. **40**, 673 (2022).
[19] R. Azim, M. T. Islam, Prog. Electromagn. Res. **133**, 391 (2013).
[20] A. Abbas, N. Hussain, M. J. Jeong, J. Park, K. S. Shin, T. Kim, N. Kim, Sensors **20**, 777 (2020).
[21] S. Yadav, A. K. Gautam, B. K. Kanaujia, Microw. Opt. Technol. Lett. **58**, 1494 (2016).
[22] J. F. Zurcher, F. E. Gardiol, Broadband Patch Antennas, 1st Edn., Artech House, 1995.
[23] R. Azim, T. Alam, M. S. Mia, A. F. Almutai, M. T. Islam, Scientific Reports **11**, 1529 (2021).
[24] M. S. Talukder, M. Samsuzzaman, M. T. Islam, R. Azim, M. Z. Mahmud, M. T. Islam, Chin. J. Phys. **72**, 310 (2021).
[25] Federal Communication Commission, FCC 2002, Docket no. 98-153.
[26] M. S. Ellis, Heliyon **7**, e08554 (2021).
[27] L. Sumana, E. F. Sundarsingh, S. Priyadharshini, IEEE Trans. Compon. Packag. **11**, 3 (2012).
[28] O. P. Kumar, P. Kumar, T. Ali, Micromachines **13**, 12 (2022).
[29] Z. Wang, X. Liu, N. Rasool, Z. Tang, F. Chen, Electron. Lett. **58**, 747 (2022).
[30] Z. Chao, Z. Zitong, X. Pei, Y. Jie, L. Zhu, L. Gaosheng, Scientific Reports **12**, 19703 (2022).
[31] M. D. Geyikoglu, Analog Integr. Circuits Signal Process. **114**, 439 (2023).

* Corresponding author: rezaulazim@cu.ac.bd